ELSEVIER

Ceramics International 29 (2003) 61–68

CERAMICS INTERNATIONAL

www.elsevier.com/locate/ceramint

Densification of ashes from a thermal power plant

E. Benavidez*, C. Grasselli, N. Quaranta[1]

Desarrollo y Tecnología de Materiales, Facultad Regional San Nicolás, Universidad Tecnológica Nacional, Colón 332 (2900), San Nicolás, Argentina

Received 20 March 2002; received in revised form 2 May 2002; accepted 5 June 2002

Abstract

Power plants generate a great amount of solid waste named ash during coal combustion. From this process two different kinds of ashes are extracted: fly ash (FA) and bottom ash (BA). In this work possible use of both fly and bottom ash as raw material for the ceramic industry, is analyzed. The samples were formed by mechanical mixing of both kinds of ashes, and density evolution during conformation as structural ceramic (packing, pressing and sintering) was studied. It was verified that powders with larger fly ash content exhibited higher packing density resulting in compacts with improved green and sintered densities. Preheating treatments at temperatures above 600 °C also increased the green and sintered densities. Dilatometric curves on compacts formed from FA and BA powders were run at constant heating rate and at isothermal cycles. From the analysis of these data it can be established that liquid-phase sintering is the densification mechanism present at 1180 °C.

Keywords: Fly ash granules; Recycling; Densification

1. Introduction

Significant amounts of solid wastes are produced during combustion of coal in thermal power plants. This residue is known as ash (unburned material) and can be classified according to the zone where it is recovered from. Thus, two kinds of ash are distinguished: fly ash (FA) and bottom ash (BA). About 80% of the ash is entrained in the gas flow and it is captured and recovered as fly ash. The remaining 20% of the ash is bottom ash, a dark gray, granular, and porous material, whose particle size is predominantly below 12.7 mm, which is collected in a water-filled hopper at the bottom of the furnace. When a given amount of bottom ash drops into the hopper, it is removed, conveyed and stockpiled for disposal.

The fly ash can be classified as class F, normally produced from burning anthracite or bituminous coal, or class C, normally produced from lignite or subbituminous coal [1]. The first one (aluminosilicate ash) has pozzolanic properties and the second one (calcium sulphate ash) has both pozzolanic and some cementitious properties [1].

Fly ash utility and applications have intensively studied in industrial countries. Owing to the environmental problem, each region develops specific studies about the characterization and use of their own ashes.

At present, there is an intensive search to increase their uses, although they are utilized as raw materials in the cement industry [2–4] where they are mixed with clays and carbonates. Besides, they have been used for land filling, which is an unsatisfactory solution from both ecological and economical points of view [5]. Other uses of residual ashes as raw material in the brick and ceramic tile fabrication, as filler in plastics and paints, and for metal recovery have been proposed [6]. The fly ashes were combined with sodium aluminates to synthesize zeolites [7], and it was suggested that fly ash can be converted into tobermorite [8] which can be used in the separation, immobilization and disposal of radioactive species such as cesium and strontium.

On the other hand, some studies to incorporate the fly ash as ceramic raw material have been made owing to the high percentage of silica and alumina contained in class F. For example, zirconia was added to a fly ash matrix in some proportions, up to 25% ZrO_2, and a strong interaction of Al_2O_3, ZrO_2 and Fe_2O_3 with SiO_2 to form mullite, zircon and faylite, respectively was noticed [9]. The possible formation of mullite phase

* Corresponding author. Fax: +54-3461-420820.
E-mail address: ebenavidez@frsn.utn.edu.ar (E. Benavidez).
[1] CICPBA Researcher.

0272-8842/02/$22.00
PII: S0272-8842(02)00090-1

from sintering reaction of fly ash and alumina was analyzed [10]. In this study the lowest porosity and the highest microhardness were present in samples heated at 1500 °C with 30 and 40% alumina. In other work, both classes F and C fly ashes were used to synthesize mullite [11]. Owing to the high levels of impurities present in class C fly ash they were not suitable to obtain mullite. However, class F fly ash, with a previous beneficiation process, reached a complete mullitization at 1600 °C (2 h) with an ash:alumina ratio of 115:100. This clean ash-derived mullite presented water absorption, density, refractoriness, thermal expansion coefficient and fracture toughness comparable with commercial mullite.

Fly ashes were mixed with float dolomite (waste from zinc mineral extraction) to obtain amorphous glasses at 1550 °C [12]. These glasses were recrystallized into partially crystallized materials (glass ceramics). Both the original glasses and the glass ceramics showed better thermal and mechanical properties than the conventional glasses and/or commercial glass ceramics [12].

The preparation of glass matrix composite materials was reported by Boccaccini et al. [13], the matrix was formed by fly ash and cullet glass (obtained from float glass production). Alumina platelets were used as reinforcement material, and the fly ash content was varied between 10 and 90% by weight. The mechanical properties (Young's modulus, bending strength, hardness and toughness) increased when platelets content increased, although the porosity in the samples was high. Alumina platelets reinforcement permitted to obtain materials with low brittleness index (less brittle) that would result in a material having good machinability.

Know-how on the ash compacting characteristics was presented by Guo et al. [14,15] who mixed fly ash and aluminum powders to produce low cost composite materials with potential applications in the automotive industry. The authors described the preparation of aluminum–fly ash composite materials by the conventional compacting and sintering route.

The aim of this work is to determine the possible use of both fly ash and bottom ash as raw materials for the ceramic industry. Here an initial study to know packing and compacting characteristics of fly and bottom ashes and their influence on the final density of the compacts is presented. The thermal evolution of shrinkage by dilatometric measurements is described.

2. Experimental procedure

The starting materials were ashes produced during the coal combustion in a thermal power station. They were classified in bottom ash (BA) and fly ash (FA). Both kind of powders were dried at 100–110 °C to reach a constant weight.

Particle size distributions were determined by dry sieving (ASTM C92-76). In the BA powder particles higher than 1.70 mm (agglomerates retain on mesh 12) were excluded because they were too large and they produced some difficulties during the compacts conformation process. These agglomerates constitute between 15 and 18 wt.% of BA powder, while there is not a detectable presence of this particle size in the FA powder.

Both types of ashes, without previous calcination treatment (samples NP), were mechanically mixed with three weight ratios FA/BA = 1/3, 1 and 3. Additional samples were obtained from the powders FA, BA and FA/BA = 1 precalcined during 2 h at 350 °C (samples P350), 600 °C (samples P600) and 880 °C (samples P880).

The morphology of different ashes was examined by scanning electron microscopy (SEM) in a Philips 505 microscope, and elemental analysis was determined by energy dispersive analysis (EDS).

Residual coal contained in the ashes was determined from the mass loss after 6 h at different temperatures in the range 400–1000 °C.

Packing density (ρ_p) was obtained weighting the powder poured into a cylindrical container. The ρ_p was calculated using the mass:volume ratio (picnometric determination). The ρ_p values presented here are averages of five measurements.

A 1 wt.% of polyvinyl alcohol (PVA) was added as binder to ash powders. PVA was dissolved in distilled water previously to its addition to the powder. Approximately 1 g of powder was uniaxially cold pressed at 100 MPa. A cylindrical matrix, 12.0 mm in diameter, was used and compacts resulted among 3.9–6.1 mm in height.

The green density (ρ_o) of the compacted powders was calculated from the mass:volume ratio, determining geometrically the volume of compacts.

Different compacts were heated during 2 h at 1100, 1150 and 1200 °C. The sintering density (ρ_s) was calculated by the immersion method using distilled water.

Some compacts forming from FA and BA powders were assayed in a dilatometer (Theta Instruments Inc., Dilatronic II). The samples were heated, at 5 °C/min constant rate, up to different isothermal temperatures: 1100, 1150 and 1200 °C, where they were maintained for 2 h. All thermal treatments were performed under normal atmospheric conditions.

3. Results

3.1. General characteristics of the ashes

Chemical analysis of BA and FA ashes by EDS determination (wt.% of oxides) is shown in Table 1.

Table 1
Chemical composition of bottom ashes (BA) and fly ashes (FA) in weight percentage of oxides

Oxides	BA	FA
SiO_2	57.7	56.0
Al_2O_3	21.5	24.4
Fe_2O_3	9.5	7.3
CaO	7.1	7.2
TiO_2	2.3	2.8
MgO	1.1	1.4
K_2O	0.8	1.0

These data show that silica (SiO_2) and alumina (Al_2O_3) are the main oxides. Besides, both ashes have an important amount of iron oxide (as ferric) and calcium oxide.

Chemical compositions of both the FA and the BA ashes are similar, but an important difference from the residual coal content in each one is observed. The residual coal is approximately 2.5 wt.% in FA powders, while this percentage rises to 11.5 wt.% in BA powders. As it is shown in Fig. 1, the highest mass loss ($\Delta m/m_o$) is produced below 500 °C.

Fig. 2a shows typical morphology of FA powders. In this SEM image spherical particles with a broad particle size distribution are observed. Such spherical shape was observed throughout this sample.

Angular particles are observed in the SEM micrograph of Fig. 2b corresponding to BA powder. Besides agglomerates of spherical particles were present in this sample. As it was already explained the different zones of burner where the ashes are removed determine the shape of the particles.

Sample obtained from FA and BA powders mixed in equal proportions (FA/BA = 1) presents both angular and spherical particle shapes as it is shown in Fig. 2c and d. In this powder, block-like particles greater than 10 μm are observed. These blocks are rounded by spherical particles brought principally by FA powder.

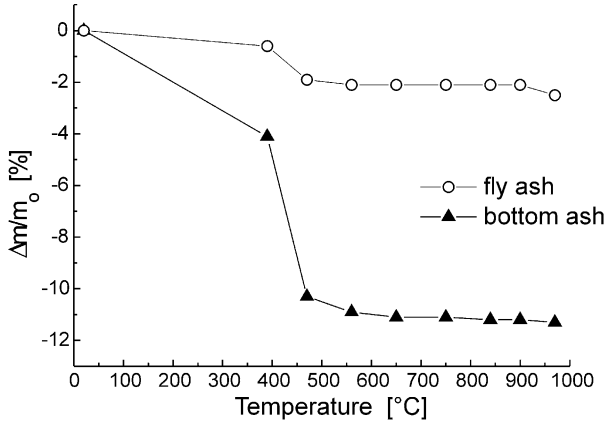

Fig. 1. Percentage of mass loss in the fly ash and bottom ash powders at different temperatures.

The particle size distributions of the ashes without calcination process and precalcined at 600 °C are presented in Fig. 3. The NP bottom ash powder has 22.0 wt.% of particles lower than 75 μm (Fig. 3a). On the other hand, the amount of this finer particles increases until 74.5 wt.% in the NP fly ash powder (Fig. 3b).

As it can be observed from these figs. when the FA and BA powders are heated at 600 °C, the distribution of particle size changes. Fraction lower than 75 μm increases its weight percentage in both precalcined ashes. In the bottom ashes this increase is also present in fraction between 75 and 150 μm. On the contrary, the weight percentage in the fly ashes 75–150 μm decreases when they are precalcined at 600 °C, and the residual coal in the as received ashes is eliminated.

From these results, it was observed that the FA powder presents three principal differences with respect to the BA one: (1) a lower residual coal content, (2) more particles with spherical shape, and (3) finer particle size distribution.

3.2. Packing grade and densification

The influence of residual coal on both the packing grade and densification process was evaluated. Packing density, green density and final sintering density in samples from powders NP, P350, P600 and P800 were compared.

Fig. 4a shows packing densities of different powders, produced by mixing FA and BA powders without precalcination treatment (NP). It can be noticed that an increase in the FA content permits to obtain a powder with higher packing densities. This behavior has influence on compacts densities, provided that samples with higher packing densities attain higher green densities, and higher green density leads to higher final density when the compact is sintered at 1200 °C during 2 h.

The same behavior was observed in samples formed from ashes preheated at 350 °C (Fig. 4b), 600 °C (Fig. 4c) and 880 °C (Fig. 4d).

In Fig. 5, it can be observed that there is no significant difference among green densities of compacts formed with NP and P350 powders. However, a considerable increase in these densities is observed in compacts formed from BA and FA/BA powders when these are preheated at 600 and 880 °C.

Dilatometric curves from compacts formed by fly and bottom ashes are shown in Fig. 6 where Lo is the initial length of the compacts. It can be seen that there is not contraction for temperatures below 700 °C. For BA compact, shrinkage starts at 725 °C, while for FA compact, densification starts at 760 °C. From 800 to 1070 °C an important length contraction of both compacts is produced. Thus, at 1070 °C the shrinkage is about 7%

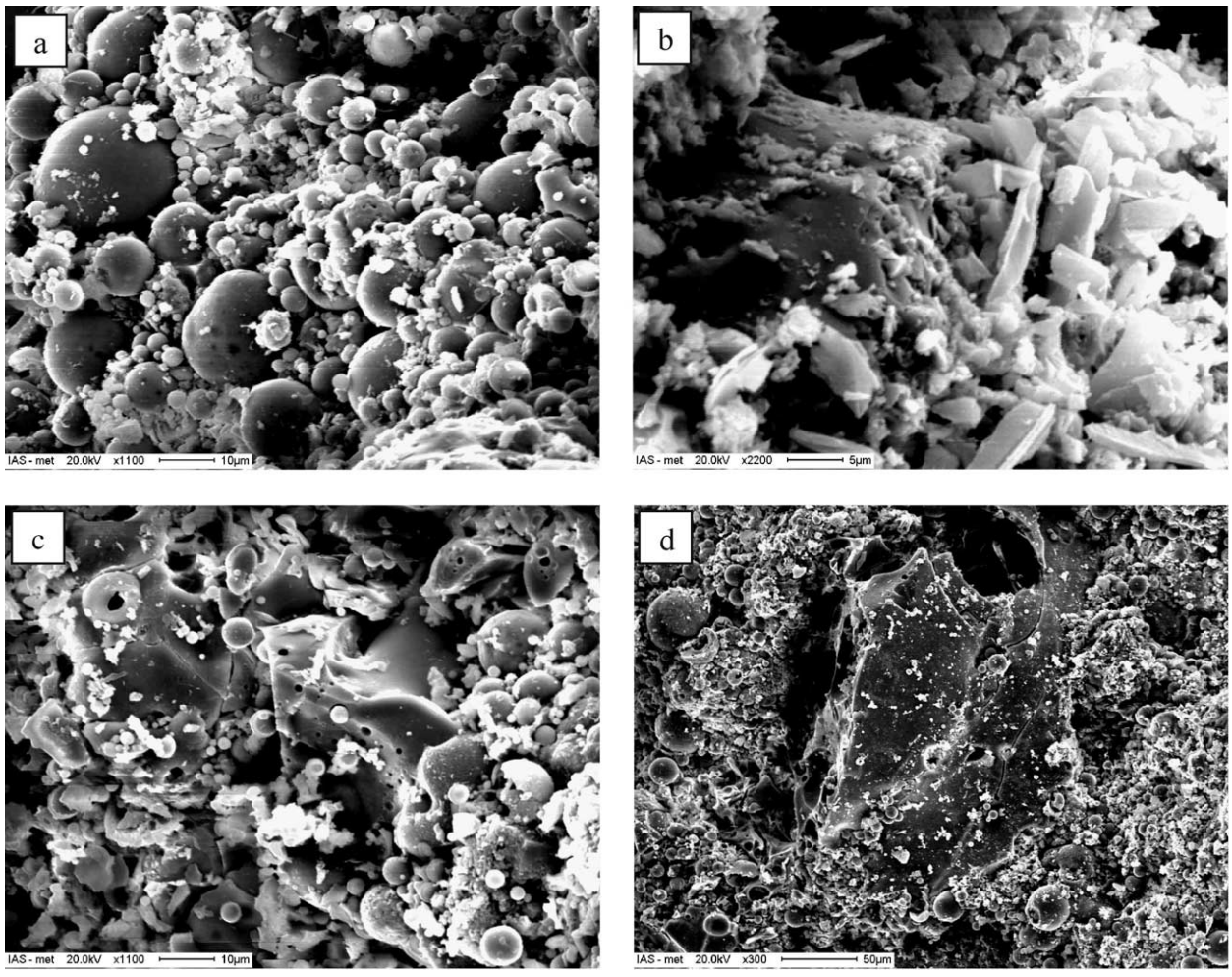

Fig. 2. SEM images of (a) FA powders, (b) BA powders and (c)–(d) mixed powders with ratio FA:BA = 1.

in the FA compact and 6% in the BA one. In the interval of temperature between 1070 and 1180 °C shrinkage is stopped forming a plateau in the dilatometric curve. Then when the temperature exceeds 1180 °C a new contraction cycle is initiated.

In Fig. 7, shrinkage curves of both compacts described above are presented as a function of isothermal time. When the isothermal cycle is started the time is $t = 0$, thus the negative values in the time axis correspond to the heating cycle setup at 5 °C/min. These curves show that the shrinkage of FA compact stops at 1100 and 1150 °C, consistent with dilatometries performed at constant heating rate as it was seen in Fig. 6. It was observed that after 6 h under isothermal treatments at 1100 °C and at 1150 °C the sample remained without change (not shown here). However, after 2 h at 1200 °C, the FA and BA compacts attained an additional shrinkage of ≈5%. Thus, both types of compacts suffered a total contraction of ≈12%.

An analysis on the isothermal curves was realized to determine the time exponent (n). This exponent affects the shrinkage according to the equation: $\Delta L/Lo = K(T, r, \gamma, D) \cdot t^n$, where t is the time at the sintering temperature and K is a constant depending on: the temperature (T), the particle size (r), the surface tension (γ), and the diffusion coefficient of the mechanism involved in the sintering process (D). The value of time exponent can be associated, from theoretical models, to different densification mechanisms. In Fig. 8 the ln(shrinkage) versus ln(time) curves from the dilatometric data presented in Fig. 7 are shown. In this case the initial height of compacts (Lo) is taken at start of isothermal cycle ($t = 0$).

These curves can be fitted by straight lines, and their slopes permit to calculate the exponent n. As it is observed in this fig. the curves can be fitted by two straight lines, r1 and r2 (continuous lines are drawn to visual help). In Table 2, the ordinate to origin ($\ln K$) and the slope (n), corresponding to r1 and r2, are shown.

According to the values of Table 2, during the first 5 or 6 min the shrinkage of these compacts at 1200 °C can be fitted by an exponent $n \approx 1$. From 10 min in BA compact or 14 min in FA compact, the time exponent $n \approx 1/3$ and this value continues until the final of isothermal cycle (120 min).

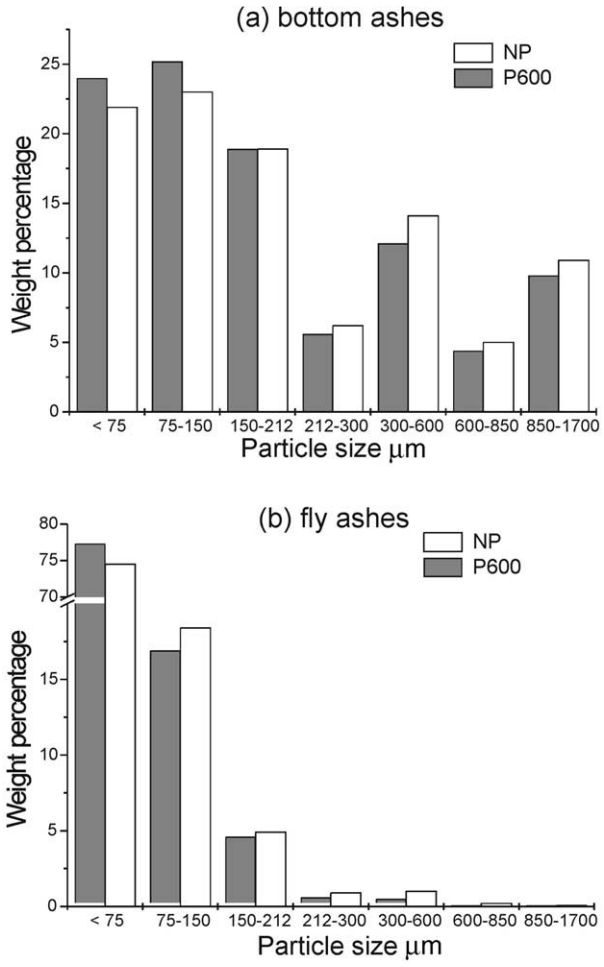

Fig. 3. Particle size distribution corresponding to as received and precalcined at 600 °C powders of (a) bottom ashes and (b) fly ashes.

4. Discussion

From the earlier results, three important differences between FA and BA samples are noted, (1) the residual coal content, (2) the morphology of particles, and (3) the particle size distributions. The bottom ashes contain a greater amount of coal thus determined by a greater loss mass during heating (see Fig. 1). Besides, this material presents a wider particle size distribution and a higher percentage of particles with size upper than 75 μm. These properties have influence on the stacking density of powders and green and sintering densities of compacts.

Table 2
Coefficients of linear fittings corresponding to r1 and r2

Fit	ln K	n	t (min)
r1—FA	7.42	1.10	1 – 6
r1—BA	8.17	0.95	0.5 – 5
r2—FA	9.02	0.36	14 – 120
r2—BA	0.45	0.29	10 – 120

Although the precalcined treatments do not show influence on the packing density, the powders precalcined at $T > 350$ °C produced compacts with both higher green density and higher sintering density. The increase in ρ_o and ρ_s it can be attributed to two reasons. First, a lower ρ_s in compacts formed by ashes without preheating process (NP) or preheated at 350 °C (P350) would be produced removing the residual coal present in the samples. This coal is eliminated as carbon gas products generating pores in the compacts. As a result a greater porosity is present in the NP and P350 samples formed by bottom ashes (see Fig. 5) because these powders contain a greater residual coal content. Second, in a previous work, Chu et al. [16] has probed that a precoarsening heating treatment produced a narrower particle size distribution. This behavior can also be seen in Fig. 3: the particle size distributions of FA and BA precalcined powders have a tendency to concentrate in smaller particle sizes. On the other hand, the precoarsed samples in Chu et al. [16] attained a greater final density relative to compacts without precoarsening treatment. The P600 compacts were formed by powders calcined below the densification temperature (see Fig. 6), while the P880 compacts were formed from powders treated at a temperature where some densification grade took place. In this work, there is no influence on the ρ_o and ρ_s densities of the compacts formed from BA and FA/BA = 1 powders, but in compacts from FA powders there is an increase in the ρ_s value from 1.80 to 1.87 g/cm^3, corresponding to P600 and P880, respectively. It must be reminded that, according to Fig. 1, the mass loss at 600 and 880 °C were similar. Thus, in both P600 and P880 compacts, the residual carbon in the powders has totally been removed.

The samples densities at different stages (powder packing, green compact and sintered compact) determined that the greater content of fly ash causes both greater powder and compact densities. The higher green density can be attributed to a better spatial distribution (stacking) of the particles when the powder is poured into the matrix. This greater packing grade is due both to a more spherical morphology of fly ash and a particle size distribution that is concentrated in sizes lower than 75 μm. Then, it is known by previous works [17,18] that a greater green density promotes a greater density of the sintered compact. Besides, as it was noted above, the lower residual coal content in FA powder will produce a lower porosity during its thermal evolution. On the other hand, it is possible to think that the space among particles (pores) generated into the powders is smaller when smaller is the particles size. Then, the smaller pores are easier to eliminate during heating than the bigger ones. By this reason, the lower size of the FA powders allows to obtain compacts with lower porosity. Although it has not been probed which is the grade of influence by each mechanism on compact densities, all

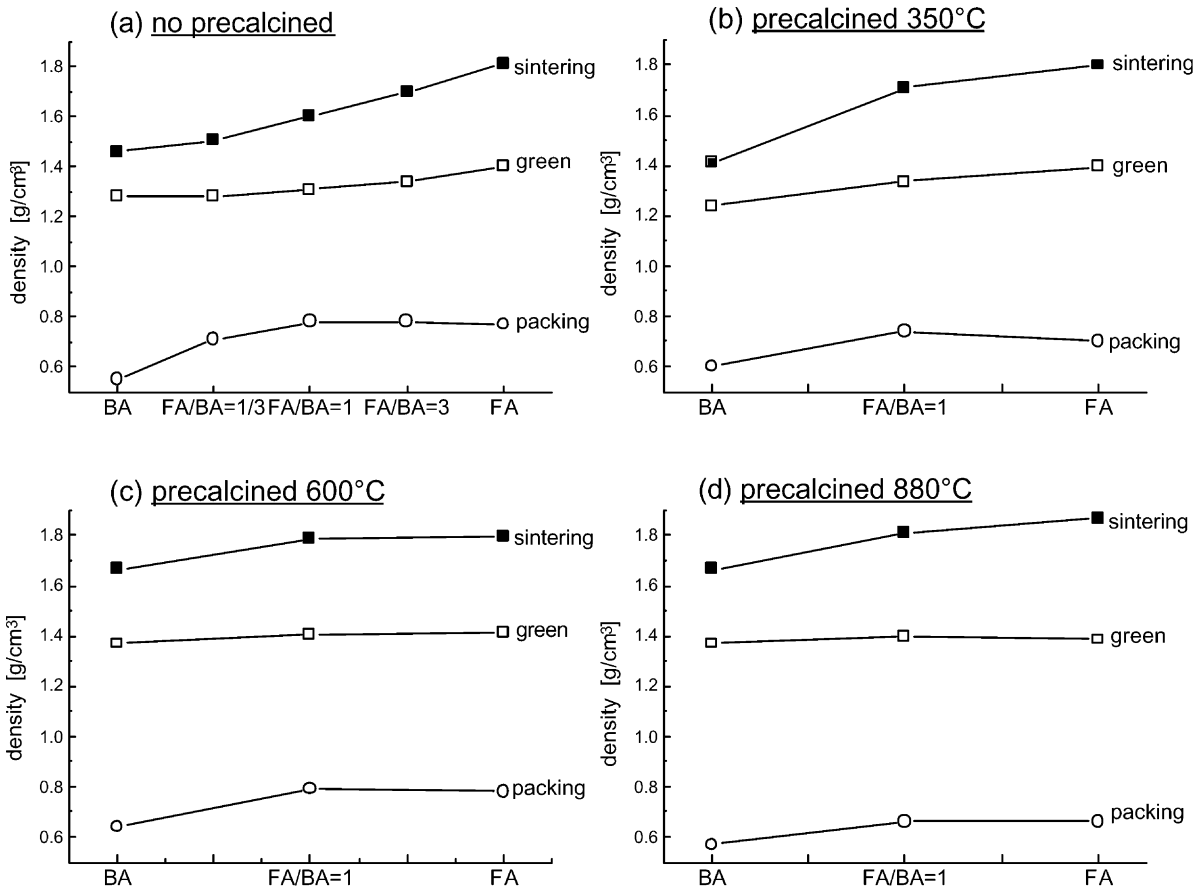

Fig. 4. Packing, green and final densities of samples FA, BA and FA/BA = 1, formed from powders NP and precalcined at 350, 600 and 880 °C.

these facts tend to confirm that the fly ash characteristics produce more dense compacts. The highest density (1.87 g/cm^3) was obtained in the sample prepared from FA powders precalcined at 880 °C, according to the previous discussion. However, the samples prepared with the ratio FA:BA = 1, and precalcined at 600 and 880 °C, presented also good density values: ρ_s(P600) = 1.79 g/cm^3 and ρ_s(P880) = 1.81 g/cm^3, respectively.

Densification started at 725 °C in bottom ash compact and at 760 °C in fly ash compact. The more angular morphology of BA is, probably, the reason of sharp

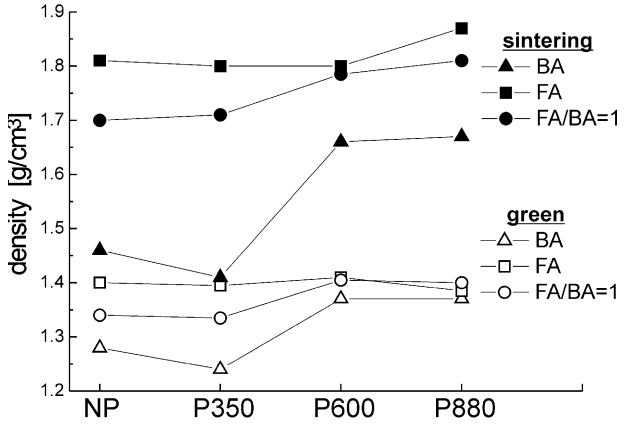

Fig. 5. Green and sintering densities of FA, BA and FA/BA = 1 compacts formed from NP, P350, P600 and P880 ash powders.

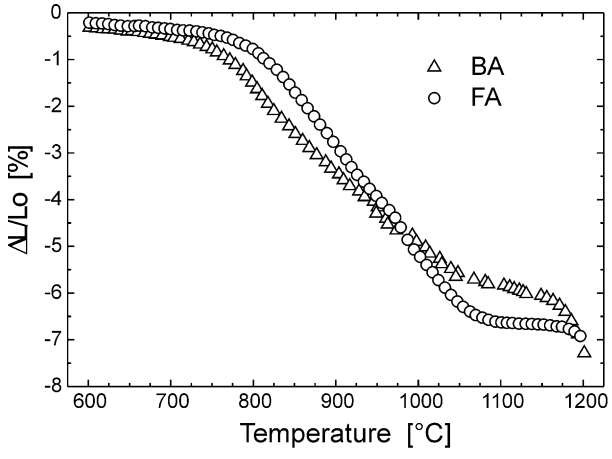

Fig. 6. Shrinkage curve of the FA and BA compacts heated at constant rate of 5 °C/min up to 1200 °C.

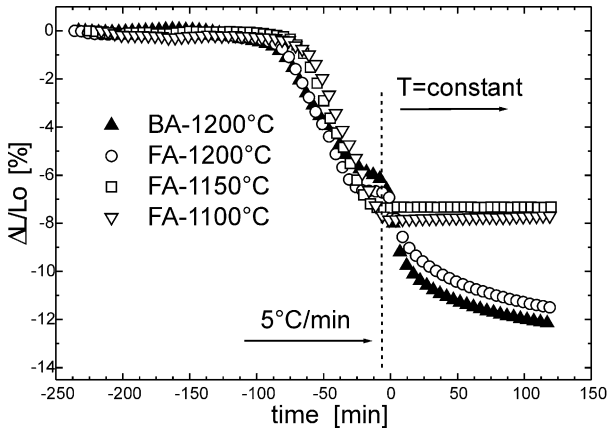

Fig. 7. Dilatometric curves during heating and isothermal cycle of fly ash and bottom ash compacts.

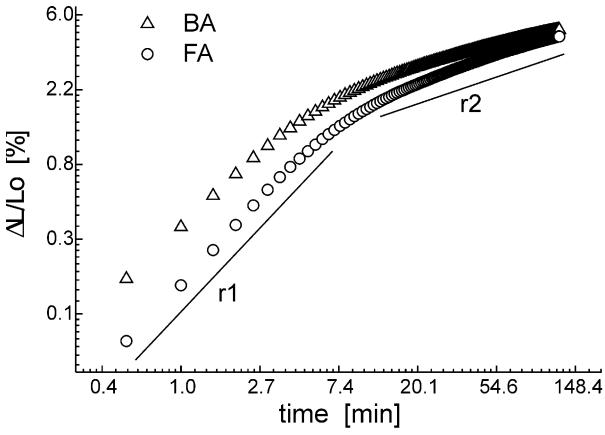

Fig. 8. Curves corresponding to ln(ΔL/Lo) versus ln(time) used to calculate the time exponent.

contact points among particles. Those contacts determine the interparticle neck formation (initial stage of sintering) at a lower temperature.

Evidently, there are two densification stages at high temperatures (>600 °C). The first stage operates in the 800–1070 °C range and the second one at temperatures upper than 1180 °C (see Fig. 6). Between both densification periods, from 1070 °C to 1180 °C, the compacts present a very low shrinkage.

At temperatures above 1180 °C, the mechanism of densification can be determined analyzing its time behavior at 1200 °C. From theoretical models it is known that time exponent $n = 1$ is related to rearrangement process, which is present when a liquid phase is in contact with ceramic grains [19,20]. Besides, the time exponent $n = 1/3$, from 10 minutes to 120 min in the isothermal cycle, corresponds to solution-precipitation process. This stage, following the Kingerys' model [11], appears after the rearrangement stage. Thus, it can be established that the densification process observed above 1180 °C in the ash compacts, is caused by sintering assisted by a liquid phase.

5. Conclusions

The present study showed that it is possible to obtain dense sintered compacts starting from powders that were previously mixed in the same amounts from fly and bottom ashes. These powders had been precalcined at 600 and 880 °C. The highest density was obtained in a sintered compact which was formed from fly ash powder precalcined at 880 °C.

The highest final density of sintered compacts is directly related with a lower residual coal content, narrower particle size distribution and higher "sphericity" of the fly ash particles.

From time dependence of the compact shrinkage during its thermal processing, it can be concluded that at temperatures higher than 1180 °C the grains densification is controlled by the presence of a liquid phase. During isothermal dilatometry at 1200 °C, the rearrangement of the grains is present at the first minutes and then the solution–precipitation process is established.

Acknowledgements

The authors gratefully acknowledges Mr. Edmundo González, from IAS (Instituto Argentino de Siderurgia) for SEM images and Central Térmica San Nicolás for the supplied material.

References

[1] Annual Book of ASTM Standards. Standard specification for Fly Ash and Raw or Calcined Natural Pozzolan for Use as a Mineral Admixture in Portland Cement Concrete, vol. 04.02, ASTM, Philadelphia, PA, USA, 1992, C 618–92a, pp. 306–308.
[2] G.L. Jablonski, S.S. Tyron, Overview of coal combustion by-product utilization, in: Proceedings of the 5th International Pittsburg Coal Conference, University of Pittsburgh, PA, USA, 1988, pp. 15–21.
[3] J. Olek, Dynamic/static modulus of elasticity and Poisson's ratio of flyash concrete, in: A.M. Brandt, V.C. Li, I.H. Marshall (Eds.), Proceedings International Symposium on Brittle Matrix Composites 4, IKE and Woodhead Publ, Warsaw, 1994, pp. 425–436.
[4] Y. Erel, A. Matthews, Y. Nathan, Potential use of coal ash in the Israel Cement Industry, Cement and Concrete Res. 18 (1988) 503–512.
[5] C.L. Carlsson, D.C. Adriano, Environmental impacts of coal combustion residues, J. Environ. Qual. 22 (1993) 227–247.
[6] J.-Y. Hwang, X. Huang, A.M. Hein, Synthesizing mullite from beneficiated fly ash, JOM 47 (5) (1994) 36–39.
[7] M.W. Grutzeck, D.D. Siemer, Zeolites synthesized from class F fly ash and sodium aluminate slurry, J. Am. Ceram. Soc. 80 (9) (1997) 2449–2453.
[8] W. Ma, P.W. Brown, S. Komarneni, Sequestration of cesium and strontium by tobermorite synthesized from fly ashes, J. Am. Ceram. Soc. 79 (6) (1996) 1707–1710.
[9] L.N. Satapathy, The physical, thermal and phase identification studies of zirconia–flyash material, Ceram. Int. 24 (1998) 199–203.

[10] N. Quaranta, S. Camelli, M. Caligaris, E. Benavidez, R. Caligaris, A.R. Boccaccini, H. Kern, Processing of mullite ceramics using fly ash and alumina, in: G. Müller (Ed.) Proceedings of the EUROMAT 99, vol. 12, Wiley-VCH, Weinheim, 2000, pp. 184–188.
[11] X. Huang, J.Y. Hwang, B.C. Mutsuddy, Properties of mullite synthesized from fly ash and alumina mixture, Interceram 44 (2) (1995) 65–71.
[12] L. Barbieri, T. Manfredini, I. Queralt, J.M. Rincon, M. Romero, Vitrification of fly ash from thermal power stations, Glass Technology 38 (5) (1997) 165–170.
[13] A.R. Boccaccini, M. Bücker, J. Bossert, K. Marszalek, Glass matrix composites from coal flyash and waste glass, Waste Management 17 (1) (1997) 39–45.
[14] R.Q. Guo, P.K. Rohatgi, D. Nath, Compacting characteristics of aluminium–fly ash powder mixtures, J. Mater. Sci. 31 (1996) 5513–5519.
[15] R.Q. Guo, P.K. Rohatgi, D. Nath, Preparation of aluminium–fly ash particulate composite by powder metallurgy technique, J. Mater. Sci. 32 (1997) 3971–3974.
[16] M-Y. Chu, L.C. De Jonghe, M.K.F. Lin, F.J.T. Lin, Precoarsening to improve microstructure and sintering of powder compacts, J. Am. Ceram. Soc. 74 (11) (1991) 2902–2911.
[17] F.F. Lange, Sinterability of agglomerated powders, J. Am. Ceram. Soc. 67 (2) (1984) 83–89.
[18] M.N. Rahaman, L.C. De Jonghe, M. Chu, Effect of green density on densification and creep during sintering, J. Am. Ceram. Soc. 74 (3) (1991) 514–519.
[19] W.D. Kingery, Densification during sintering in the presence of a liquid phase. I, Theory, J. Appl. Phys. 30 (3) (1959) 301–306.
[20] A. Mortensen, Kinetics of densification by solution–reprecipitation, Acta Mater. 45 (2) (1997) 749–758.